Optics Communications 371 (2016) 226–230

Contents lists available at ScienceDirect

Optics Communications

journal homepage: www.elsevier.com/locate/optcom

Optimal focusing conditions of lenses using Gaussian beams

Juan Manuel Franco [a], Moisés Cywiak [a,*], David Cywiak [b], Idir Mourad [c]

[a] Centro de Investigaciones en Óptica, A.C., Loma del Bosque No. 115, León Gto, Mexico
[b] Centro Nacional de Metrología, Querétaro 76246, México
[c] Brookhaven National Laboratory – NSLS II 50 Rutherford Dr. Upton, 11973-5000 New York, USA

ARTICLE INFO

Article history:
Received 5 December 2015
Received in revised form
16 February 2016
Accepted 28 March 2016
Available online 2 April 2016

Keywords:
Best focusing plane
Focal length
Focusing lens
Fresnel number

ABSTRACT

By using the analytical equations of the propagation of Gaussian beams in which truncation exhibits negligible consequences, we describe a method that uses the value of the focal length of a focusing lens to classify its focusing performance. We show that for different distances between a laser and a focusing lens there are different planes where best focusing conditions can be obtained and we demonstrate how the value of the focal length impacts the lens focusing properties. To perform the classification we introduce the term delimiting focal length. As the value of the focal length used in wave propagation theory is nominal and difficult to measure accurately, we describe an experimental approach to calculate its value matching our analytical description. Finally, we describe possible applications of the results for characterizing Gaussian sources, for measuring focal lengths and/or alternatively for characterizing piston-like movements.

1. Introduction

It is well known that there is a difference in the calculation of a focused field when it is performed by means of ray tracing compared to physical optics. It has been found a shift between the geometrical focus position and the one obtained using diffractive models. Contrary to geometrical optics, physical optics demonstrated that the plane of better focusing moves closer to the aperture of the lens [1–6]. Calculations on the value of the focal-shift as a function of the Fresnel number for a focused spherical wave with a spatial Gaussian profile can be found in [7]. A study of the focal shift by a thin lens on a weakly-truncated Gaussian beam as a function of a low Fresnel number has been studied in [8]. Spherical converging waves as a function of the Fresnel number, particularly when it is less than one were carried out in [9]. In [10] it was found that the axial intensity distribution is not symmetrical around the geometrical focus. In [11,12] the focal shift is determined as a function of an effective Fresnel number and again the shift is towards the lens. Numerical studies have also been carried out in which a dependence of the wavelength is included and it was found that as the geometric focal length increases, the Fresnel number decreases and the focal shift is magnified [13].

However, to the best of our knowledge, no calculations have been provided involving the value of the focal length in conjunction with the distance of propagation between the laser and the lens. These calculations are essential when setting up an experiment, for example a lens with short focal length can be used for focusing purposes at a certain distance from the laser and later, for different experimental requirements, it may be necessary to replace the lens by one with a larger focal length working at a different distance. For setting up properly the experiment, it is more useful to know the consequence of changing both parameters. In this report, we describe the effect of this change on the focusing conditions.

In the following sections we will use well-known analytical equations, based on the scalar Fresnel diffraction integral, that allow us to classify the behavior of a focusing lens as a function of its focal length, the distance between the lens and the waist plane and the wavelength. We show that the plane where best focusing conditions are obtained follows a specific locus. This locus results to be a function of the wavelength and the semi-width of the beam at the waist plane as described in the following sections.

2. Analytical description

Fig. 1 describes the physical situation. The waist of a laser beam with a circularly-symmetric Gaussian intensity profile is located at a coordinate plane (x_0, y_0), referred as the Gaussian waist plane. A thin focusing lens with a focal length f is placed at a distance z_0 at a coordinate plane (ξ, η). The plane of observation is placed at a distance z_1 at a coordinate plane (x_1, y_1) at the back of the focusing lens.

* Corresponding author.
E-mail address: moi@cio.mx (M. Cywiak).

http://dx.doi.org/10.1016/j.optcom.2016.03.084
0030-4018/

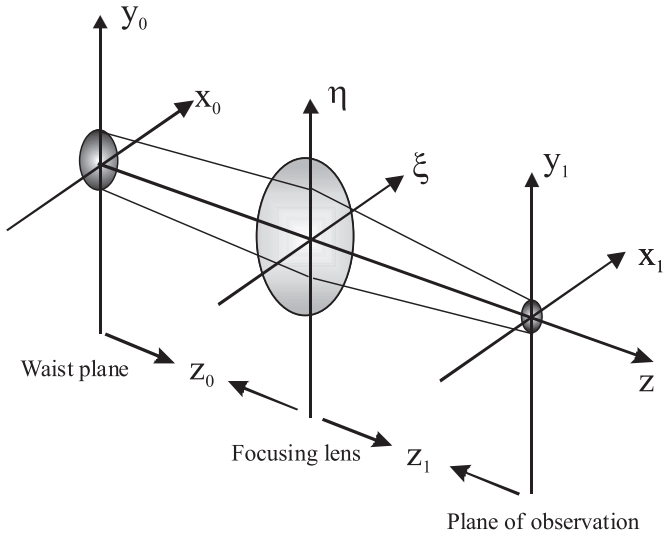

Fig. 1. Physical situation as described in the text.

At the Gaussian waist plane, the amplitude distribution of the field at (x_0, y_0) is represented by,

$$\Psi(x_0, y_0) = A\exp\left(-\frac{x_0^2 + y_0^2}{r_0^2}\right). \tag{1}$$

In Eq. (1) A is a constant, not important for our description, and r_0 is the semi-width of the Gaussian beam.

The amplitude distribution at the coordinate plane (ξ, η), just before the lens, calculated using the Fresnel diffraction integral, is a diverging Gaussian beam described by,

$$\Psi_1(\xi, \eta) = A\exp\left(-\frac{\xi^2 + \eta^2}{r_1^2}\right)\exp\left(i\pi\frac{\xi^2 + \eta^2}{\lambda R_1}\right), \tag{2}$$

where r_1 is the semi-width of the beam,

$$r_1 = \frac{1}{\pi r_0}\sqrt{\lambda^2 z_0^2 + \pi^2 r_0^4}, \tag{3}$$

and R_1 its corresponding radius of curvature,

$$R_1 = \frac{1}{\lambda^2 z_0}(\lambda^2 z_0^2 + \pi^2 r_0^4). \tag{4}$$

The amplitude distribution just after the lens is given by Eq. (2) multiplied by the quadratic phase term $\exp(-i\pi\frac{\xi^2+\eta^2}{\lambda f})$, introduced by the lens.

The amplitude distribution at the plane of observation with coordinates (x_1, y_1) can be calculated again using the Fresnel integral and is also a Gaussian distribution,

$$\Psi_F(\xi, \eta) = A_F\exp(-\frac{x_1^2+y_1^2}{r_F^2})\exp(i\pi\frac{x_1^2 + y_1^2}{\lambda R_F}), \tag{5}$$

where the semi-width r_F is given as,

$$r_F(z_1) = \frac{1}{\pi r_1 R_1 f}\sqrt{(\lambda z_1 R_1 f)^2 + \pi^2 r_1^4 (z_1 f + R_1 f - R_1 z_1)^2}, \tag{6}$$

and the radius of curvature as,

$$R_F(z_1) = \frac{(\lambda R_1 z_1 f)^2 + \pi^2 r_1^4 (z_1 f + R_1 f - R_1 z_1)^2}{z_1(\lambda R_1 f)^2 + \pi^2 r_1^4 (z_1 f + R_1 f - R_1 z_1)(f - R_1)}. \tag{7}$$

We have previously reported (Eqs. (3)–7) in [14].

The radius of curvature given by Eq. (7) is irrelevant for the present description and its analytical expression is given for completeness.

Using Eqs. (3–4) and $z_1 = f$ in Eq. (6) gives,

$$r_F = \frac{\lambda f}{\pi r_0}. \tag{8}$$

Eq. (8) stands for the well-known fact that regardless of the distance between the laser and the focusing lens (z_0), the semi-width of the beam at the back-focal plane takes always a constant value which is not necessarily a minimum. As indicated by Eq. (6) r_F is a function of the position of the plane of detection (z_1). The value z_1 that gives the minimum semi-width can be obtained by calculating the derivative of r_F with respect to z_1 and this value corresponds to the position of the plane where the beam exhibits a minimum semi-with. We will refer to this plane as the best focusing plane (BFP) and its position is given as,

$$z_{Opt} = \frac{\pi^2 r_1^4 R_1 f(R_1 - f)}{(\lambda R_1 f)^2 + \pi^2 r_1^4 (R_1 - f)^2}. \tag{9}$$

In Eq. (9), z_{Opt} will be referred as the best focusing distance (BFD). The corresponding semi-width at z_{Opt} is obtained by substituting this value in Eq. (6) as,

$$r_{Opt}(z_{Opt}) = \frac{1}{\pi r_1 R_1 f}\sqrt{(\lambda z_{Opt} R_1 f)^2 + \pi^2 r_1^4 (z_{Opt} f + R_1 f - R_1 z_{Opt})^2}. \tag{10}$$

It can be noticed that Eq. (10) depends on (Eqs. (3) and 4) which in turn are functions of z_0.Thus, the semi-width r_{Opt} can be plotted as a function of z_0 and z_{Opt} in a single graph; we will refer to such a graph as the locus of the BFP. Two loci are illustrated in Figs. 2 and 3 for two different lenses, one with a relatively short 5.0 cm focal length and the other one with an 81.0 cm focal length. The plots are calculated for $\lambda = 632.8$ nm and $r_0 = 0.44$ mm which correspond to a typical commercially available He–Ne laser.

In Figs. 2 and 3 $z_0 \approx 0$ corresponds to experimentally positioning the lens as close as possible to the waist plane. However, as Eq. (4) diverges at $z_0 = 0$, for numerically completing the locus at $z_0 \approx 0$ it is possible to choose small values on the order of some micrometers where the equation still remains valid, without reflecting appreciable changes on the value of r_{Opt}; for our calculations we used 1 μm.

From Figs. 2 and 3, two important characteristics can be extracted.

First, as z_0 increases the position of the BFP first moves away from the focusing lens until a maximum position is reached. As z_0 continues increasing the position of the BFP begins to move

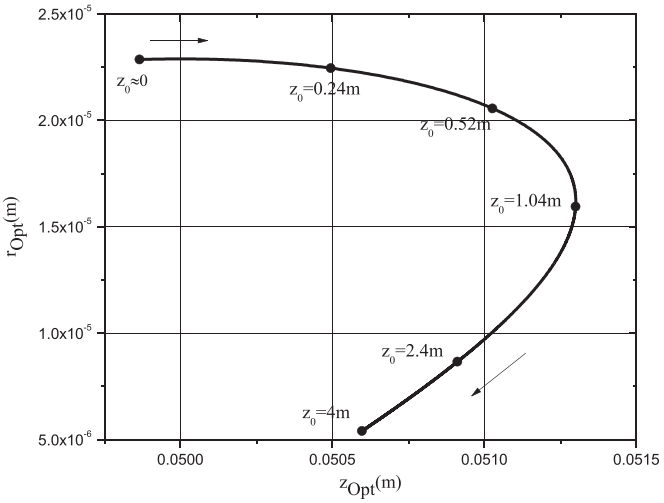

Fig. 2. Locus of the BFP for a 5.0 cm focal length lens; $z_0 \approx 0$, 0.24, 0.52, 1.04, 2.4, 4.0 m; $\lambda = 632.8$ nm, $r_0 = 0.44$ mm.

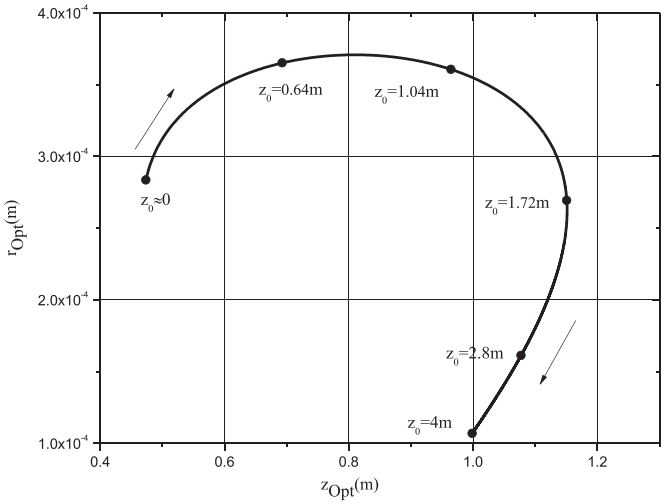

Fig. 3. Locus of the BFP for an 81.0 cm focal length lens; $z_0 \approx 0$, 0.64, 1.04, 1.72, 2.8, 4.0 m; $\lambda = 632.8$ nm, $r_0 = 0.44$ mm.

towards the lens. This property holds for both lenses.

The second characteristic marks a difference between the two lenses. For the case of the 5.0 cm lens, the semi-width at the BFP always decreases as z_0 increases. In contrast, for the 81.0 cm lens, as z_0 starts to increase, the semi-width at the BFP also increases up to a maximum value and then decreases.

From the best of our knowledge, the two characteristics described above have not yet been reported. In previous reports the propagation from the waist-plane towards the lens a distance z_0 has not been considered. For tuning properly an experimental arrangement, this propagation results relevant.

An alternative way to appreciate the change of the semi-width for the case of the 81.0 cm lens is by plotting r_{Opt} as a function of z_0, as illustrated in Fig. 4.

In Fig. 4, the semi-width at the BFP exhibits a maximum at approximately $z_0 = 80$ cm. In this case the maximum value is approximately 1.3 times the value of the semi-width at $z_0 \approx 0$. As a consequence, increasing the distance between the focusing lens and the waist plane will not result in a better focusing as can be seen from Figs. 3 and 4. There is a distance range away from the lens in which a widening of the beam results, contrary to what intuitively may be expected.

At this point, it is necessary to establish a criterion to classify the lenses by means of the value of their focal length. We define the term delimiting focal length of a lens, denoted f_K, as the one where the semi-width on the BFP exhibits a maximum increase of 30% as compared with the semi-width at $z_0 \approx 0$; i.e. an increase of 1.3 times of the semi-width at $z_0 \approx 0$. For descriptive purposes, the value 1.3 is selected rather arbitrarily. In particular the focal length of 81.0 cm chosen in the above example is precisely the delimiting focal length for $\lambda = 632.8$ nm, $r_0 = 0.44$ mm.

It is possible to find an appropriate relation of f_K as a function of λ and r_0 by means of Eq.(10), which, as indicated, requires (Eqs. (3) and 4) which are functions of z_0. For this, we build a table of r_{Opt} as a function of z_0, providing a guess value for f in the referred equations, and maintaining r_0 and λ constant. From this table, we record two values, the one that corresponds to r_{Opt} for $z_0 \approx 0$, that will be referred as $r_{Opt}(0)$, and the maximum value of r_{Opt} in the table which will be referred as r_{Max}. Next, the ratio $r_{Max}/r_{Opt}(0)$ is calculated. If this ratio differs from 1.3, the table is discarded and a new table is built by trying a different guess value. This process is repeated until the desired ratio is obtained. When this condition is obtained, the value assigned to f corresponds to f_K. Fig. 4 represents graphically the table that corresponds to the value f_K.

To obtain a plot of f_K as a function of λ, we used the above procedure for different values of λ ranging from 0.1 to 4.0 μm, maintaining $r_0 = 0.44$ mm. Fig. 5 shows the obtained plot. In the plot dots represent discrete values obtained by the described procedure and the solid line represents a fitting of the data.

As previously indicated, the value r_0 was maintained constant. To calculate f_k as a function of r_0, we repeated the above procedure for different values of r_0 ranging from 0.1 mm to 0.6 mm. From the obtained data, it is possible to fit an equation of the form,

$$f_k(r_0, \lambda) = \frac{A(r_0)}{\lambda} + B(r_0). \tag{11}$$

Figs. 6 and 7 show corresponding plots to the functions given by Eq. (11).

In Figs. 6 and 7, dots represent data obtained with the analytical procedure. As we have mentioned, a corresponding equation was fitted for each plot and represented as continuous traces respectively.

With the fitted equations, Eq. (11) can be written approximately as,

$$f_k(r_0, \lambda) = \frac{(2.28\, r_0^{1.98} - 2.23 \times 10^{-9})}{\lambda} + (7.5 \times 10^3 r_0^2 - 4.5\, r_0 + 3.74 \times 10^{-4}). \tag{12}$$

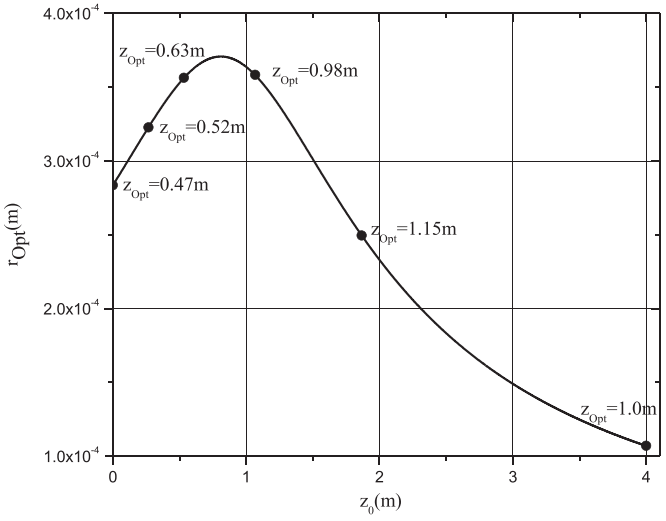

Fig. 4. r_{Opt} as a function of z_0 for the 81.0 cm lens.

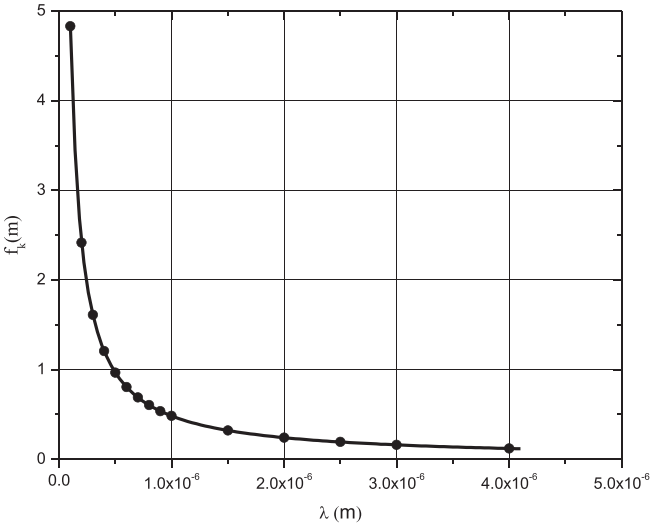

Fig. 5. f_k as a function of λ for $r_0 = 0.44$ mm.

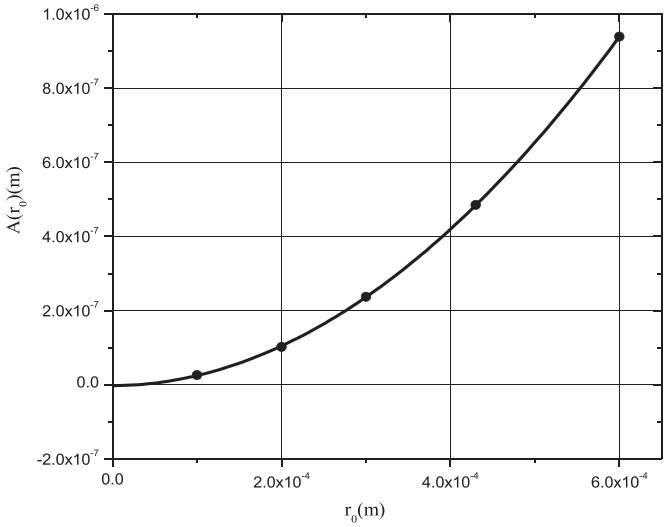

Fig. 6. $A(r_0)$ as a function of r_0.

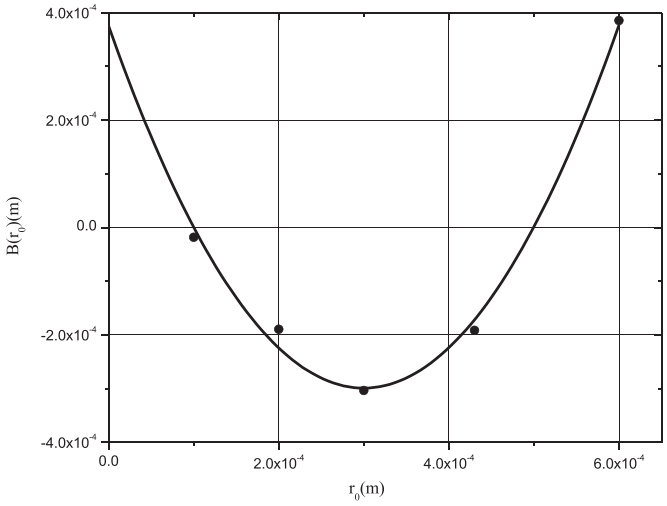

Fig. 7. $B(r_0)$ as a function of r_0.

Eq. (12) can be used to estimate the value of f_K with reasonable accuracy by knowing the wavelength and the semi-width of the Gaussian waist. For instance, for our experimental setup, substituting $r_0=0.44$ mm, $\lambda=632.8$ nm, gives $f_k(r_0, \lambda)\approx 0.81$ m as anticipated.

To experimentally verify the approximation given by Eq. (12), we used a lens of focal length 80 cm, which is commercially available and has a value near f_K (81 cm) for our laser. We placed the lens at two different positions, first, as closed as possible of the output of the laser and then at a distance of approximately 80 cm from the output. The semi-widths at the respective BFPs were measured. As anticipated, approximately 1.3 increase on the semi-width was measured. To further verify Eq. (12) for different values of λ and r_0 experiments with different lasers have to be performed. As indicated, Eq. (12) was obtained in a range of λ between 0.1 and 4 μm and r_0 from 0.1 to 0.6 mm.

For the case of a source exhibiting a different spatial distribution, it should be possible to represent it by a superposition of Gaussian wavelets; however, additional research is required in this direction.

In a previous report [14], we have demonstrated experimentally the accuracy of the equations applied to a real lens, we have also described how to obtain the BFP locus by means of a knife-edge homodyne profilometer especially devised for this purpose. However, it has not yet been explicitly determined the value of f for a real lens. In the following section we describe a procedure to determine the value of f that fits appropriately with the analytical equations. In general, this value does not coincide with the one reported by the lens manufacturer, and neither with the one used in other reports. Once this value has been obtained, the system may then be used to experimentally characterize piston-like movements by means of Gaussian beams.

3. Experimental section

To determine f experimentally we will make use of a well-known effect. If the plane of observation is placed at a position just behind the focusing lens and then moved away from the lens, the beam under inspection will exhibit an excursion that ranges from a focusing region up to a diverging one. This effect can be calculated by using Eq. (6) which is a function of z_0 as it depends on (Eqs. (3) and 4). Fig. 8 shows plots of the semi-width at the plane of observation when it is moved at different distances z_1 from just behind the lens up to a distance of approximately 0.8 m. The semi-width at each plane is plotted as a function of z_1 for large values of z_0. Three values around $z_0=2.0$ m, are plotted. The plots correspond to a lens with a focal length of 20.0 cm that we have arbitrarily chosen to be used in our experimental set up. The value of the focal length chosen to carry this measurement is unimportant since the behavior of the plots is similar regardless of the value of the focal length; thus, the method can be applied to any focusing lens.

Precisely just behind the lens, when z_1 is small, the semi-width for each curve corresponds approximately to the value r_1 given by Eq. (3); this value is imposed by the divergence of the laser. As z_1 increases the semi-width decreases up to a minimum that corresponds to the one in the BFP and can be determined from its corresponding locus. Further increasing z_1 will result in increasing semi-widths.

The procedure to measure f consists in fixing a constant distance z_1 for the plane of observation, i.e., to fix the distance between the lens and the plane of observation This distance z_1 must be away from the focal region, in our experiment we have selected $z_1=0.4$ m. With z_1 fixed, we now proceed to change the distance z_0 in a range away from the laser source and registering the semi-width for each position z_0. In Fig. 9 dots correspond to the experimental data measured in a range of z_0 from 2.0 to 9.0 m. The continuous lines were obtained by using the analytical (Eqs. (3),

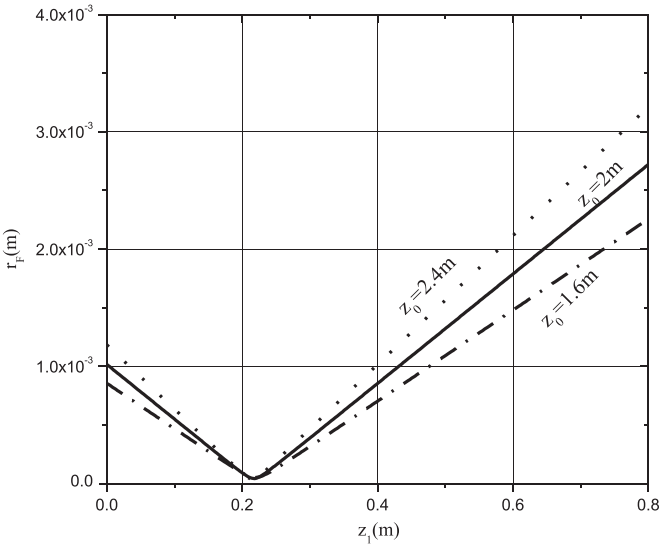

Fig. 8. Plots for the 20.0 cm focal length lens for $z_0=1.6$, 2.0 and 2.4 m.

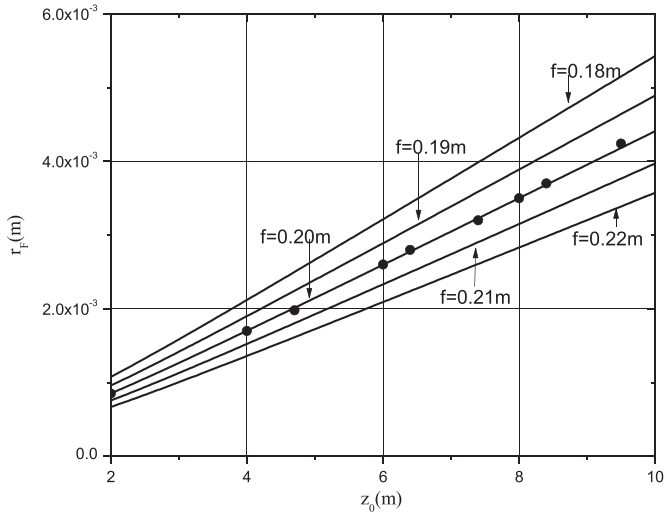

Fig. 9. Beam semi-width as a function of z_0 for $z_1 = 0.4$ m. $\lambda = 632.8$ nm, $r_0 = 0.44$ mm. Dots correspond to experimental data. The continuous lines are obtained by using the analytical equations as referred in the text.

4) and (6) with $z_1 = 0.4$ m for 5 different values of f ranging from 0.18 to 0.22 m. It can be noticed that the value $f = 0.2$ m fits well with the experimental data. As predicted by the analytical equations a linear response is obtained, and from this response the value of f can easily be determined; this value corresponds to the one given in the quadratic phase lens.

Once the laser source and the focal length are characterized, the plots can be applied, for example, in characterizing piston-like movements by fixing a mirror to the surface of the moving object and using a fast camera for determining the semi-width in real time.

4. Conclusions

We have examined characteristic loci of focusing lenses using analytical equations of Gaussian beams. We found that there are two different loci which depend on the value of the focal length affecting the focusing behavior at best focusing conditions. From the loci differences, the term delimiting focal length was defined and used to characterize focusing properties of lenses. Once a lens has been properly characterized, the model can be applied to characterize Gaussian sources or piston-like displacements.

Acknowledgments

We thank CONACyT for partial support.

References

[1] J.J. Stamnes, D. Velauthapillai, Focal shifts on focusing through a plane interface, Opt. Commun. 282 (12) (2009) 2286–2291.
[2] Ari T. Friberg, et al., Focal shifts of converging diffracted waves of any state of spatial coherence, Opt. Commun. 196 (1) (2001) 1–7.
[3] Yajun Li, Dependence of the focal shift on Fresnel number and f number, J. Opt. Soc. Am. 72 (6) (1982) 770–774.
[4] M. Parker Givens, Focal shifts in diffracted converging spherical waves, Opt. Commun. 41 (3) (1982) 145–148.
[5] G.D. Sucha, W.H. Carter, Focal shift for a Gaussian beam: an experimental study, Appl. Opt. 23 (23) (1984) 4345–4347.
[6] Yajun Li, Emil Wolf, Focal shifts in diffracted converging spherical waves, Opt. Commun. 39 (4) (1981) 211–215.
[7] Jakob J. Stamnes, Waves in Focal Regions: Propagation, Diffraction and Focusing of Light, Sound and Water Waves, CRC Press, Boca Raton 1986, pp. 336–337.
[8] Yajun Li, Focal shift formula for focused, apertured Gaussian beams, J. Mod. Opt. 39 (8) (1992) 1761–1764.
[9] C.J.R. Sheppard, P. Török, Dependence of focal shift on Fresnel number and angular aperture, Opt. Lett. 23 (23) (1998) 1803–1804.
[10] T.C. Poon, Focal shift in focused annular beams, Opt. Commun. 65 (6) (1988) 401–406.
[11] William H. Carter, Focal shift and concept of effective Fresnel number for a Gaussian laser beam, Appl. Opt. 21 (11) (1982) 1989–1994.
[12] M. Martınez-Corral, C.J. Zapata-Rodrıguez, P. Andrés, E. Silvestre, Effective Fresnel-number concept for evaluating the relative focal shift in focused beams, J. Opt. Soc. Am. A 15 (2) (1998) 449–455.
[13] G. Zhou, Focal shift of focused truncated Lorentz-Gauss beam, J. Opt. Soc. Am. A 25 (10) (2008) 2594–2599.
[14] Franco S. Juan Manuel, Moisés Cywiak, David Cywiak, Idir Mourad, Experimental profiling of a non-truncated focused Gaussian beam and fine-tuning of the quadratic phase in the Fresnel Gaussian shape invariant, Opt. Commun. 355 (2015) 74–79.